

Effect of Ag Layer Thickness and Interference of Cu-SnO₂/Ag/Cu-SnO₂ (CTO/Ag/CTO) Multilayer Thin Film on the Electrical and Optical Properties

Anju Dutt^{a,b*}, Sangeeta^{a,b}, Harpreet Singh^{a,b} & Anand Kumar^a

^aDepartment of Physics, Institute of Integrated and Honors Studies, Kurukshetra University, Kurukshetra, Haryana 136 119, India

^bDepartment of Physics, Kurukshetra University, Kurukshetra Haryana 136 119, India

Received 7 July 2023; accepted 4 August 2023

The present study reports the successful fabrication of CTO/Ag/CTO multilayer thin films with different sandwiched layer (Ag) thickness on a glass substrate by the E-beam evaporation Method. The influence of sandwiched layer thickness and stacking of layers on electrical and optical properties was investigated. Several analytical tools such as X-ray diffraction, Atomic Force microscopy, Hall Effect measurement, and UV-visible spectroscopy were used to investigate the morphological, electrical, and optical properties of the multilayer thin film structure. Multilayer thin film with 14nm Ag thickness exhibited a good combination of conductivity and transmittance (*i.e.* $4.64 \times 10^4 \Omega^{-1}\text{cm}^{-1}$, 69.3%). The conduction mechanism can be explained on the basis of the islands growth mechanism of Volmer-weber model as Ag film was grown on an amorphous CTO surface. The Haacke's figure of merit was calculated for valuing the overall performance of the transparent conducting film. The maximum figure of merit is reported as $8.7 \times 10^{-3} \Omega^{-1}$ for multilayer thin film having Ag thickness of 14nm.

Keywords: Multilayer thin films; Electrical properties; Optical properties; Conduction mechanism

1 Introduction

The combination of high conductivity and good transparency of transparent conducting oxides (TCO) has increased interest in the area of optoelectronics devices¹⁻³. The Oxide/metal/Oxide multilayer thin film structures have been vigorously considered. Doped metal oxides such as Aluminium doped ZnO⁴, Indium doped tin Oxide⁵, and Niobium doped tin Oxide⁶ have been investigated as top and bottom layers in multilayer thin film structures because of their ease of manufacturing and brilliant properties. In the present study, we used Copper doped Tin Oxide (CTO) as a top and bottom layer due to its low resistivity and high transmittance. Also, it has low-cost and easy availability. Here, Ag metal was favoured for sandwiched layer since it shows low sheet resistance and high transmittance in the visible region of light⁷. The thickness of sandwiched layer and deposition circumstances can play a significant role in achieving the optimal balance between optical and electrical properties.

In the present study, CTO/Ag/CTO multilayer thin films were deposited by the E-beam evaporation method on a glass substrate at different temperatures.

A detailed study of the electrical and optical properties of single layer, bilayer, tri-layer, and the interference among them has been presented. The effect of sandwiched layer thickness on the electrical and optical properties of multilayer thin film structure has also been investigated.

2 Materials and Methods

To fabricate CTO/Ag/CTO multilayer thin film structure, firstly glass substrates were cleaned with liquid soap, distilled water, acetone and isopropyl alcohol for 15 min each and dried in an oven. The CTO pellet and Ag metal chunks were used as target materials for E-beam evaporation. Initially, Cu-doped SnO₂ powder was prepared by solid state reaction method using commercially available SnO₂ (99% pure) and CuO (99% pure) materials. These were mixed together in a fixed ratio (98 mol% of SnO₂ and 2 mol% of Cu) and grinding was done for 2hrs in a mortar pestle to get fine powder. The CTO pellets of 14mm diameter were prepared using a hydraulic machine under pressure 50kg/cm² and annealed at 950 °C. Deposition of CTO and Ag layer thin film was done by E-beam evaporation method at a pressure of 2×10^{-5} mbar with a deposition rate of 0.3Å/sec and substrate rotation rate of 10rpm. For,

*Corresponding author: (E-mail: anju.ihs@kuk.ac.in)

CTO/Ag/CTO multilayer thin film, a layer of CTO was initially deposited by keeping the voltage, current and substrate temperature at 5 kV, 40mA and 200 °C, respectively. Thereafter, the Ag layer was deposited by keeping the voltage, current and substrate temperature at 5 kV,7mA and 30 °C, respectively and thereafter CTO layer was again deposited. The thicknesses of the films were controlled by using a quartz crystal thickness monitor fitted within the evaporation chamber. The thickness of the top and bottom layer of CTO was fixed to 30nm and the thickness of the mid layer *i.e.*, Ag layer was varied as 8nm, 10nm, 12nm, and 14nm. The samples of CTO single layer, CTO/Ag(10nm) bilayer, CTO/Ag(10nm)/CTO tri-layer, CTO/Ag(8nm)/CTO,CTO/Ag(12nm)/CTO, and CTO/Ag(14nm)/CTO are represented as CTO1, CTO2, CTO3, CTO4, CTO5, and CTO6, respectively, for simplicity.

The crystallinity of the multilayer thin film samples was confirmed by Bruker D8 Advanced X-ray diffractometer taking measurements at a glancing angle of 0.2°. The surface topography was studied by Atomic Force Microscope (Bruker Multimode-8 AFM) using tapping mode. The surface roughness and particle size were calculated using Gwyddion software. The optical properties were measured by UV-VIS-NIR spectroscopy (UV 3600 plus Shimadzu UV-VIS-NIR spectrophotometer). The electrical properties were determined by the Hall Effect Measurement system and four probe method. A 0.5-tesla magnetic field was applied normally to the surface of the sample and analysis was done using Ecopia software.

3 Results and Discussion

The Glancing angle X-ray diffraction patterns are shown in Fig. 1. In Fig. 1(a) the CTO1 shows an amorphous structure. In the multilayer CTO/Ag/CTO thin film X-ray diffraction pattern, the four peaks of

Ag with different intensities are obtained. A high-intensity (111) peak of silver at 38.15° and the other peaks (200), (220), and (311) of moderate intensity corresponding to 44.18°, 64.45°, and 77.6° are identified respectively. At 12nm silver layer thickness, peaks are of small intensity and one additional peak is found that may be due to some impurity present in the sample.

The average crystallite size is calculated using the Debye-Scherrer formula⁸:

$$D = K\lambda/\beta\cos\theta \quad \dots (1)$$

Where β is Full Width Half Maxima (FWHM), λ is the wavelength, K is Scherrer constant equal to 0.9, and θ is the diffraction angle. The average crystallite size is found to be in the range of 7-10nm. We have also calculated the crystallite size and microstrain using Williamson–Hall plot method⁹ and the average crystallite size of samples is found in the range of 5-7nm. The strain is observed as negative which indicates the compressive strain in the film.

The AFM micrographs are used for the analysis of surface roughness and particle size of thin films. The AFM 3D images of CTO1, CTO2, and CTO3 thin films are shown below in Fig. 2. All the films show a crack-free surface structure.

It is clear from Fig. 2(a-c) that with increasing the number of layers, RMS roughness increases from 0.050 nm to 0.162 nm.

From Fig. 3(a-d) it can be seen that with increasing the Ag layer thickness, RMS roughness decreases from 0.216nm to 0.114nm, hence smoothness increases. A smooth surface reduces the scattering of light and improves the transparency of the thin film. The particle size is also calculated using Gwyddion software and it is found to be 78nm, 154nm, 138.4nm and 105.8nm for CTO4, CTO3, CTO5, and CTO6, respectively.

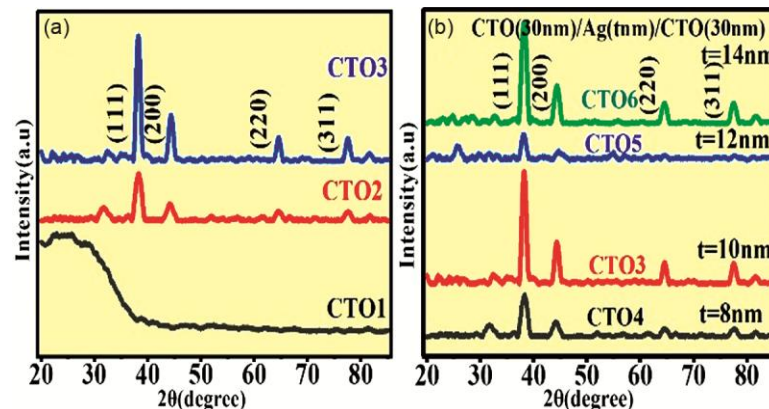


Fig. 1 — Glancing Angle X-ray Diffraction pattern of (a) CTO1, CTO2 and CTO3 samples (b) CTO4, CTO3, CTO5 and CTO6.

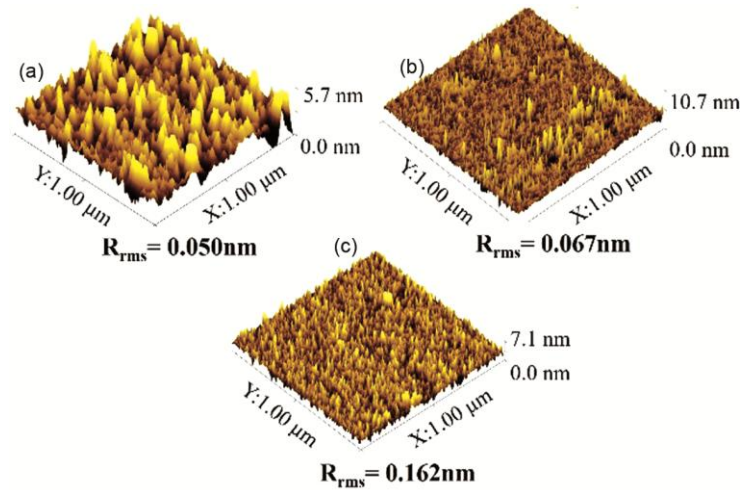


Fig. 2 — AFM 3D images with scan area $1 \times 1 \mu\text{m}^2$ (a) CTO1 (b) CTO2 (c) CTO3.

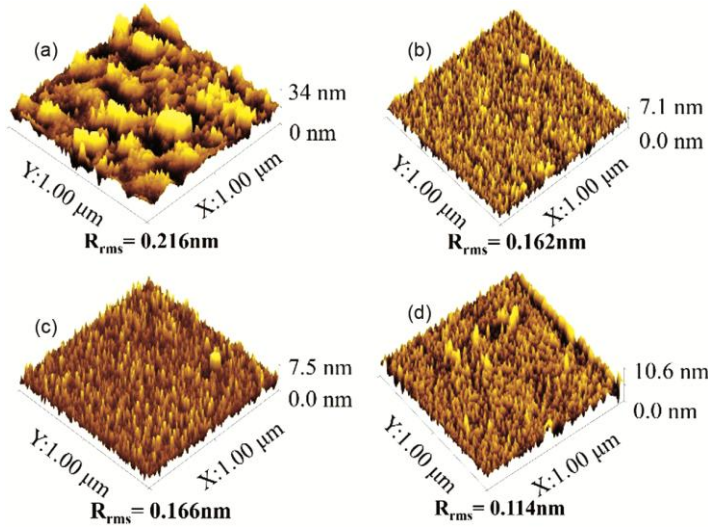


Fig. 3 — AFM 3D images with scan area $1 \times 1 \mu\text{m}^2$ of (a) CTO4 (b) CTO3 (c) CTO5 (d) CTO6.

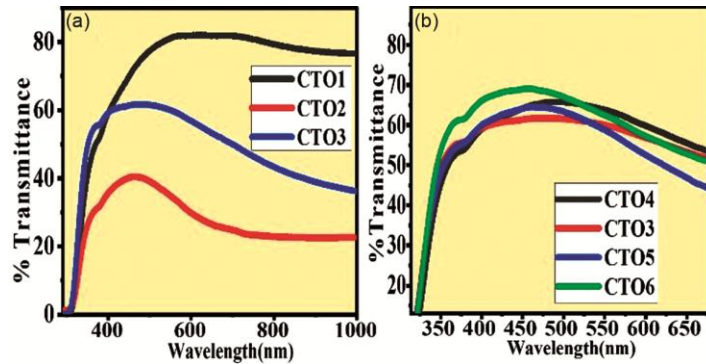


Fig. 4 — Optical transmittance spectra of (a) CTO1, CTO2 and CTO3 (b) CTO4, CTO3, CTO5, and CTO6.

The optical properties are determined by using UV-VIS-NIR spectroscopy. The optical transmittance spectra of the CTO1, CTO2 and CTO3 samples are shown in Fig. 4(a) and the value of % transmittance is

shown in Table 1. Out of three, the CTO1 shows maximum transmittance of the order of 82.5% but transmittance gets reduced to 40.5% for CTO2 due to the highly reflecting silver layer and high scattering

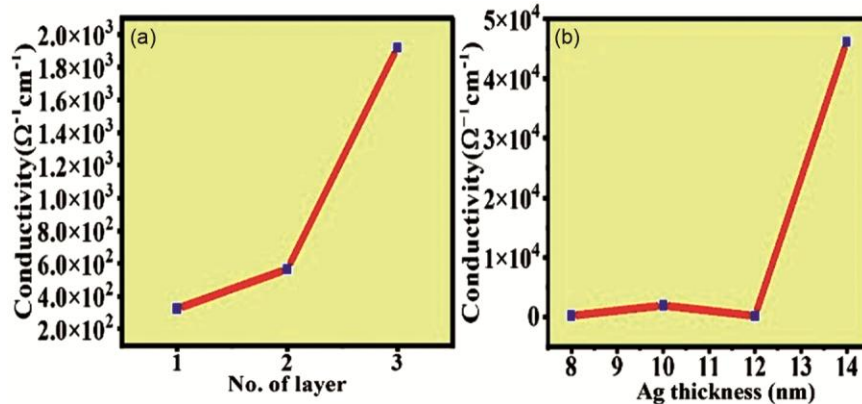


Fig. 5 —Variation of conductivity with (a) no. of stacking of layer (b) Ag layer thickness.

Table 1 — Values of % transmittance CTO1, CTO2, CTO3, CTO4, CTO5, and CTO6.

Sr. No	Samples	%T
1	CTO1	82.5
2	CTO2	40.5
3	CTO3	61.7
4	CTO4	65.9
5	CTO5	64.5
6	CTO6	69.3

losses at CTO/Ag interface. For CTO3 the transmittance comes to be 61.7%. This variation in transmittance from 82.5 to 61.7% could be due to the increase in RMS roughness as evident in Fig. 2.

The transmittance spectra of CTO4, CTO3, CTO5 and CTO6 are shown in Fig. 4(b). A sharp rise in transmittance is observed in the wavelength region from 320-370nm for all samples, thereafter, showing maxima in the 400 – 500 nm regions and then a slow decline with the increasing wavelength. The variation in maximum transmittance with Ag layer thickness is shown in Table 1.

With increasing the thickness of Ag layer from 8nm to 10nm, transmittance decreases from 65.9% to 61.7%, this can be attributed to the reflectivity of Ag layer and surface plasmon absorption¹⁰. But, as Ag layer thickness is increased from 10nm to 14nm, the transmittance increased up to 69.3%, because the continuous Ag islands decreases the scattering of light. These variations can be correlated with the variation of surface roughness.

The electrical properties are investigated using a Hall Effect measurement system. It is observed that the sheet resistance decreases from 1.03×10^3 to $7.43 \times 10^1 \Omega/\text{Sq}$ and resistivity decreases from 3.08×10^{-3} to $5.20 \times 10^{-4} \Omega\text{cm}$ with increasing the stacking of layers and corresponding conductivity increases from 3.24×10^2 to $1.92 \times 10^3 \Omega^{-1} \text{cm}^{-1}$ as shown in Fig. 5(a).

The conduction mechanism of the multilayer thin film can be described on the basis of islands growth mechanism of Volmer-Weber model¹¹, as Ag films are grown on amorphous CTO surface. The Ag layer grows in the form of islands on the CTO layer, which are discontinuous at low Ag thickness. Conduction in the discontinuous thin film through metal oxide dominates when size of the islands is very small and spaces between the islands are very large¹². There are other modes of conduction for the discontinuous film e.g. metal conduction, metal oxide conduction and quantum tunnelling. As the thickness of Ag layer increases, these islands become coalesces to form a continuous layer and then only metal conduction will be the conduction route as there is the formation of ohmic contacts between the Ag and CTO layer. Due to the favourable work function difference between them, electrons will flow smoothly from Ag layer to CTO layer¹³, therefore conductivity increases from 1.90×10^2 to $4.62 \times 10^4 \Omega^{-1} \text{cm}^{-1}$ with increase in the Ag layer thickness from 8 to 14nm as shown in Fig. 5(b). Quantum tunnelling occurs when there are larger islands with small gaps between them¹⁴. All samples showed p-type semiconducting behaviour as hall coefficient (R_H) value is found to be positive for all thin film samples.

A figure of merit¹⁵ is calculated for valuing the overall performance of the transparent conducting electrode as shown in Fig. 6.

The Haccke's figure of merit was calculated by the formula:

$$\Phi = \frac{(T)^{10}}{R_{sh}} \quad \dots (2)$$

Where T is the transmittance of multilayer thin film and R_{sh} is the sheet resistance of the thin film. The multilayer thin film CTO/Ag/CTO of 14nm of

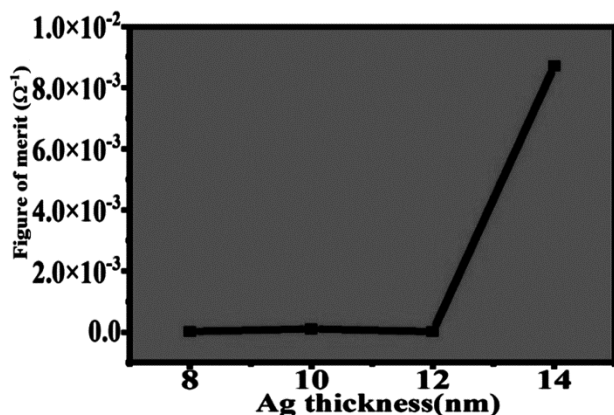


Fig. 6 — Figure of merit for the CTO/Ag/CTO multilayer thin film as a function of Ag thickness.

Ag thickness shows the best figure of merit *i.e.*, $8.7 \times 10^{-3} \Omega^{-1}$.

4 Conclusion

The multilayer thin films were successfully fabricated on the glass substrate by an electron beam evaporation method. It was observed that the large thickness of the Ag layer in a multilayer thin film improves the crystallinity of the thin film. The crystallite size is observed in the order of a few nm and the negative value of microstrain indicates the compressive strain produced in the film. After a critical layer thickness of 10nm, an increase in the transmittance with an increase in sandwiched layer thickness is observed. The conduction mechanism of the discontinuous and continuous multilayer thin film is well explained on the basis of Volmer-weber model. A good combination of high electrical conductivity and high optical transmittance is obtained at 14nm Ag layer thickness in CTO/Ag/CTO

multilayer thin film structure. A continuous multilayer thin film has shown the maximum figure of merit $8.7 \times 10^{-3} \Omega^{-1}$.

Acknowledgement

The author H.S./Sangeeta would like to acknowledge the financial support from UGC/CSIR, New Delhi (India) in the form of a SRF. The authors express their gratitude to Ion Beam Centre, Kurukshetra University Kurukshetra for providing XRD, AFM and UV-Visible Spectroscopy facilities.

References

- 1 Chopra K L, Major S & Pandya D K, *Thin Solid Films*, 102 (1983) 1.
- 2 Stadler A, *Materials*, 5 (2012) 661.
- 3 Dixon S C, Scanlon D O, Carmalt C J & Parkin I P, *J Mater Chem C*, 4 (2016) 6946.
- 4 Sahu D R, Lin S Y & Huang J L, *Thin Solid Films*, 516 (2008) 4728.
- 5 Choi K H, Kim J Y, Lee Y S & Kim H J, *Thin Solid Films*, 341 (1999) 152.
- 6 Dhar A & Alford T L, *J Appl Phys*, 112 (2012) 103113.
- 7 Han H, Theodore N D & Alford T L, *J Appl Phys*, 103 (2008) 013708.
- 8 Patterson A L, *Phys Rev*, 56 (1939) 978.
- 9 Zak A K, Majid W A, Abrishami M E & Yousefi R, *Solid State Sci*, 13 (2011) 251.
- 10 Wang P, Zhang D, Kim D H, Qiu Z, Gao L, Murakami R I & Song X, *J Appl Phys*, 106 (2009) 103104.
- 11 Lozovoy K A, Korotaev A G, Kokhanenko A P, Dirko V V & Voitsekhevskii A V C, *Surf Coat Technol*, 384 (2020) 125289.
- 12 Andersson T & Granqvist C G, *J Appl Phys*, 48 (1977) 1673.
- 13 Yu S, Zhang W, Li L, Xu D, Dong H & Jin Y, *Thin Solid Films*, 552 (2014) 150.
- 14 Biegański P, Dobierzewska-Mozrzyk E, Pieciul E & Szymczak G, *Vacuum*, 74 (2004) 211.
- 15 Haacke G, *J Appl Phys*, 479 (1976) 4086.